JPET Fast Forward. Published on November 11, 2009 as DOI: 10.1124/jpet.109.159145

Title page

Cannabidiol displays anti-epileptiform and anti-seizure properties *in vitro* and *in vivo*

Nicholas A. Jones, Andrew J. Hill, Imogen Smith, Sarah A. Bevan, Claire M. Williams, Benjamin J. Whalley and Gary J. Stephens

School of Pharmacy (NAJ, AJH, IS, SAB, BJW, GJS) and School of Psychology (CMW), University of Reading, Whiteknights, Reading, RG6 6AJ

Running title page

Running title: Cannabidiol as an anti-epileptic agent

Corresponding author:

Gary Stephens

School of Pharmacy

University of Reading

Whiteknights

PO Box 228

Reading RG6 6AJ

Tel: 44 118 378 6156

e-mail: g.j.stephens@reading.ac.uk

Number of text pages: 41

Tables: 1

Figures: 7 (+ 1 supplemental)

References: 53

Abstract: 249 words

Introduction: 515 words

Discussion: 1576 words

Abbreviations:

artificial cerebrospinal fluid (aCSF); Δ^9-tetrahydrocannabinol (Δ^9-THC); 6-nitro-7-sulphamoylbenzo(f)quinoxaline-2-3-dione (NBQX).

JPET Fast Forward. Published on November 11, 2009 as DOI: 10.1124/jpet.109.159145
This article has not been copyedited and formatted. The final version may differ from this version.

Abstract

Plant-derived cannabinoids (phytocannabinoids) are compounds with emerging therapeutic potential. Early studies suggested that cannabidiol (CBD) has anticonvulsant properties in animal models and reduced seizure frequency in limited human trials. Here, we examine the anti-epileptiform and anti-seizure potential of CBD using *in vitro* electrophysiology and an *in vivo* animal seizure model, respectively. CBD (0.01-100 μM) effects were assessed *in vitro* using the Mg^{2+}-free and 4-aminopyridine (4-AP) models of epileptiform activity in hippocampal brain slices via multi-electrode array (MEA) recordings. In the Mg^{2+}-free model, CBD decreased epileptiform local field potential (LFP) burst amplitude (in CA1 and dentate gyrus (DG) regions) and burst duration (in all regions) and increased burst frequency (in all regions). In the 4-AP model, CBD decreased LFP burst amplitude (in CA1, only at 100 μM CBD), burst duration (in CA3 and DG), and burst frequency (in all regions). CBD (1, 10 and 100 mg/kg) effects were also examined *in vivo* using the pentylenetetrazole (PTZ) model of generalised seizures. CBD (100 mg/kg) exerted clear anticonvulsant effects with significant decreases in incidence of severe seizures and mortality in comparison to vehicle-treated animals. Finally, CBD acted with only low affinity at cannabinoid CB_1 receptors and displayed no agonist activity in [^{35}S]GTPγS assays in cortical membranes. These findings suggest that CBD acts most likely in a CB_1 receptor-independent manner to inhibit epileptiform activity *in vitro* and seizure severity *in vivo*. Thus, we demonstrate the potential of CBD as a novel anti-epileptic drug (AED) in the unmet clinical need associated with generalised seizures.

Introduction

A growing number of phytocannabinoids have been shown to possess biological activity (Pertwee, 2008) and, in particular, to affect neuronal excitability in the CNS. Phytocannabinoids actions are reported to be mediated by G protein-coupled cannabinoid CB_1 and CB_2 receptors, but potentially also by other non-CB receptor targets (Howlett *et al*., 2004; Pertwee, 2008). CB_1 receptors are highly expressed in the hippocampus (Herkenham *et al*. 1990; Tsou *et al*. 1999) and are well known to modulate epileptiform and seizure activity (Shen and Thayer, 1999; Wallace *et al*., 2001). Moreover, the endocannabinoid (eCB) system has been shown to be a key determinant of hippocampal epileptiform activity (Wallace *et al*., 2002; Monory *et al*., 2006; Ludanyi *et al*., 2008). The major psychoactive compound Δ^9-THC was first phytocannabinoid reported to affect epileptiform activity; Δ^9-THC, a partial agonist at CB_1 receptors, was shown to inhibit excitatory glutamatergic neurotransmission in hippocampal neurons under low Mg^{2+} conditions (Shen and Thayer, 1999, but see Straiker and Mackie, 2005).

CBD is the major non-psychoactive component of *Cannabis sativa* whose structure was first described by Mecholaum and Shvo (1963); CBD has recently attracted renewed interest for its therapeutic potential in a number of disease states (Pertwee, 2008). CBD has been proposed to possess anticonvulsive, neuroprotective and anti-inflammatory properties in humans. Thus, within the CNS, CBD has been proposed to be protective against epilepsy, anxiety, psychosis and to ameliorate diseases of the basal ganglia, such as parkinsonism and Huntington's disease (Iuvone *et al*., 2009; Scuderi *et al*., 2009). CBD neuroprotective effects may be augmented by reported anti-oxidant properties (Hampson *et al*., 1989; Sagredo *et al*., 2007). Early studies suggested that CBD had anticonvulsant potential in one small-scale Phase I clinical trial (Cunha *et al*., 1980). In this regard, epilepsy has a significant unmet clinical need, with ~30% of epileptic

patients experiencing intractable seizures regardless of conventional AED treatment (Kwan and Brodie, 2007). CBD is extremely well tolerated in humans; for example, CBD at doses of 600 mg does not precipitate any of the psychotic symptoms associated with Δ^9-tetrahydrocannabinol (Δ^9-THC) (Bhattacharyya *et al*., 2009). At present, CBD is used therapeutically in Sativex (1:1 Δ^9-THC:CBD; GW Pharmaceuticals) to alleviate pain symptoms in multiple sclerosis and cancer pain sufferers. CBD has anticonvulsant effects in animal models of maximal electroshock Karler *et al*., 1974; Consroe and Wolkin, 1977; Consroe *et al*., 1982); however, CBD remains untested in other animal seizure models (Gordon and Devinsky, 2001) and so has yet to fulfil its indications of clinical anticonvulsant potential.

In the present study, we demonstrate the potential of CBD as an AED. We show that CBD caused concentration-related and region-dependent attenuation of chemically-induced epileptiform activity in hippocampal brain slices using *in vitro* MEA electrophysiological recordings. Furthermore, CBD reduced seizure severity and mortality in an *in vivo* model of generalised seizures. We also investigate the specific role of CB_1 receptors in CBD action and found only a low affinity interaction and lack of clear agonist effects. Overall, these data are consistent with CBD acting, most likely by CB_1 receptor–independent mechanisms, to mediate anti-epileptiform and anti-seizure effects *in vitro* and *in vivo* respectively.

Methods

In vitro electrophysiology

Tissue preparation and solutions

All experiments were carried out in accordance with Home Office regulations (Animals (Scientific Procedures) Act 1986). Acute transverse hippocampal brain slices (~450 µm thick) were prepared from male and female ($P \geq 21$) Wistar Kyoto rats using a Vibroslice 725M (Campden Instruments Ltd, UK). Slices were produced and maintained in continuously carboxygenated (95% O_2:5% CO_2) artificial cerebrospinal fluid (aCSF) composed (in mM) of: NaCl 124; KCl 3; KH_2PO_4 1.25, $MgSO_4.6H_2O$ 1; $NaHCO_3$ 36, $CaCl_2$ 2 and d-glucose 10; pH 7.4. Spontaneous epileptiform activity was induced either by exchange of the standard aCSF perfusion media for aCSF with $MgSO_4.6H_2O$ removed (Mg^{2+}-free aCSF) or by addition of the K^+ channel blocker 4-AP (100 µM) (4-AP aCSF).

Electrophysiological multi-electrode array (MEA) recording

Substrate-integrated MEAs (Multi Channel Systems, Reutlingen, Germany) (Egert *et al*., 2002a; Stett *et al*., 2003) were used to record spontaneous neuronal activity as described previously (Ma *et al*., 2008). MEAs comprised of 60 electrodes (including reference ground) of 30 µm diameter, arranged in an ~8x8 array with 200 µm spacing between electrodes. MEAs were cleaned before each recording by immersion in $5\%^{w}/_{v}$ Terg-A-Zyme (Cole-Palmer, UK) in dH_2O, followed by methanol and, finally, dH_2O before air drying. Hippocampal sections immersed in aCSF were gently micro-dissected away from surrounding slice tissue using fine forceps under a WILD M8 binocular microscope (Leica AG, Solms, Germany). Dissected hippocampi were then adhered to the cleaned MEA surface

using an applied and evaporated cellulose nitrate solution in methanol (~4 µl, 0.24%$^{w}/_{v}$; Fisher Scientific, UK) to ensure maximum contact between the tissue and recording electrodes and to avoid any physical stress upon the tissue during recordings. Slices were observed at x4 magnification with a Nikon TS-51 inverted microscope (Nikon, Japan) and imaged via a Mikro-Okular camera (Bresser, Germany) to map electrode positions to hippocampal regions. Slices were maintained at 25^{o}C, continuously superfused (~2 ml min^{-1}) with carboxygenated aCSF and allowed to stabilise for at least 10 minutes prior to recordings. Signals were amplified (1200x gain), band pass filtered (2 to 3200 Hz) by a 60 channel amplifier (MEA60 System, Multi Channel Systems) and simultaneously sampled at 10 kHz per channel on all 60 channels. Data were acquired to PC using MC_Rack software (Multi Channel Systems). Offline analysis of CBD effects upon burst amplitude, duration and frequency was performed using MC_Rack, MATLAB 7.0.4. (Mathworks Inc, Natick, MA, USA) and in-house analysis scripts. Animated contour plots of MEA-wide neuronal activity (Supplemental Fig. 1) were constructed from raw data files processed in MATLAB 6.5 using in-house code with functions adapted from MEA Tools and interpolated using a 5 point Savitzky-Golay filter in MATLAB (Egert *et al*., 2002b). These data are displayed as peak source and peak sink animation frames. Burst propagation speeds were calculated by determining burst peak times at electrode positions closest to burst initiation (CA3) and termination (CA1) sites using MC_Rack and ImageJ software (Abramoff *et al*., 2004).

Data presentation and statistics

Application of Mg^{2+}-free and 4-AP-aCSF induced spontaneous epileptiform activity characterised by recurrent *status epilepticus*-like local field potential (LFP) events (Fig. 2A,B; Fig. 4A,B). We have recently characterised and validated the use of MEA technology to screen candidate AEDs in the Mg^{2+}-free and 4-AP models using reference compounds, felbamate and phenobarbital (Hill *et al*., 2009). A discrete burst was defined as an LFP with both positive and negative components of greater than 2 standard deviations from baseline noise. In each model, LFPs were abolished by the addition of the non-NMDA glutamate receptor antagonist 6-nitro-7-sulphamoylbenzo(f)quinoxaline-2-3-dione (NBQX, 5 μM) and tetrodotoxin (TTX, 1 μM) (n=3 per model), indicating that epileptiform activity was due to firing of hippocampal neurons. Following an initial 30 mins control period, CBD was added cumulatively in increasing concentrations (30 mins each concentration). Burst parameters (amplitude, duration, frequency) were determined from the final 10 bursts of the control period or of each drug concentration. Increases in burst amplitude and decreases in frequency inherent to both *in vitro* models were observed over time in recordings in the absence of CBD (n=4 per model). These changes required appropriate compensation to allow accurate assessment of CBD effects and have been rigorously modelled by us recently (Hill *et al.*, 2009). Thus, burst frequency and amplitude from control recordings were normalised to the values observed after 30 mins of epileptiform activity, then pooled to give mean values. Curves were fitted to resultant data, and derived equations used to adjust values obtained from recordings in the presence of CBD. For amplitude; $y=0.8493*e^{(x*-0.009295)}+0.4216$ for Mg^{2+}-free- ($r^2=0.98$) and $y=0.87*e^{(-x/83.32)}+0.45$ for 4-AP- ($r^2=0.99$) induced bursting; where x = time and y = burst amplitude. Frequency changes were more complex and required fifth-order polynomial equations; $y = -9e^{-14x4} + 7e^{-10x3} – 3e^{-06}x^2 + 0.006x - 3.594$ for Mg^{2+}-free- (r^2

= 0.818); and $y = 5e^{-14x4} – 5e^{-10x3} + 2e^{-06x2} - 0.004x + 3.965$ for 4-AP- ($r^2 = 0.915$) induced bursting; where x = time and y = frequency (Hill *et al.*, 2009). Inevitable dead cell debris on the slice surface produced slice-to-slice variability in signal strength. Consequently, drug-induced changes are presented as changes to the stated measure *vs* control per experiment to provide normalised measures for pooled data. Statistical significance was determined by a non-parametric two-tailed Mann-Whitney U-test. Mean propagation speeds (m s^{-1}) were derived from pooled data and the significance of drug effects tested using a two-tailed Students t-test. In all cases, $P \leq 0.05$ was considered significant.

Pharmacology

The following agents were used: NBQX (Tocris Cookson, Bristol, UK), TTX (Alomone, Jerusalem, Israel) and 4-AP (Sigma, Poole, UK). CBD was kindly provided by GW Pharmaceuticals (Porton Down, UK). CBD was made up as a 1000–fold stock solution in dimethylsulfoxide (DMSO; Fisher Scientific, Leicestershire, UK) and stored at -20°C. Individual aliquots were thawed and dissolved in carboxygenated aCSF immediately prior to use. In all experiments, drugs were bath-applied (2 ml min^{-1}) for 30 mins to achieve steady-state effects after the induction of epileptiform activity.

Pentylenetetrazole (PTZ) in vivo seizure model

80 mg/kg pentylenetetrazole (PTZ; Sigma) was used to induce seizures in 60 adult (>P21, 70-110 g) male Wistar Kyoto rats. In the days prior to seizure induction, animals were habituated to handling, experimental procedures and the test environment. Prior to placement

in their observation arenas, animals were injected intra-peritoneally (i.p.) with CBD (1, 10 or 100 mg/kg); vehicle was a 1:1:18 solution of ethanol, Cremophor (Sigma) and 0.9% $^{w}/_{v}$ NaCl. CBD is known to penetrate the blood-brain barrier such that 120 mg/kg delivered i.p. in rats provides C_{max} = 6.8 μg/g at T_{max} = 120 minutes and, at the same dosage, no major toxicity, genotoxicity or mutagenicity were observed (personal communication via GW Pharmaceuticals Ltd; Study Report UNA-REP-02). A group of animals that received volume-matched doses of vehicle alone served as a negative control. 60 minutes after CBD or vehicle administration, animals were injected with 80 mg/kg PTZ i.p. to induce seizures. An observation system utilising closed-circuit television cameras (CCTV) (Farrimond *et al.*, 2009) was used to monitor the behaviour of up to five animals simultaneously from CBD/vehicle administration until 30 minutes after seizure induction. Input from CCTVs was managed and recorded by Zoneminder (v1.2.3; Triornis Ltd, Bristol, UK) software, then processed to yield complete videos for each animal.

Seizure analysis

Videos of PTZ-induced seizures were scored offline with a standard seizure severity scale appropriate for generalised seizures (Pohl and Mares, 1987) using Observer Video-Pro software (Noldus, Wageningen, Netherlands). The seizure scoring scale was divided into stages as follows: 0: no change in behaviour; 0.5: abnormal behaviour (sniffing, excessive washing, orientation); 1: isolated myoclonic jerks; 2: atypical clonic seizure; 3: fully developed bilateral forelimb clonus; 3.5: forelimb clonus with tonic component and body twist; 4: tonic-clonic seizure with suppressed tonic phase with loss of righting reflex; 5: fully developed tonic-clonic seizure with loss of righting reflex (Pohl and Mares, 1987).

Specific markers of seizure behaviour and development were assessed and compared between vehicle control and CBD groups. For each animal the latency (in s) from PTZ administration to first sign of seizure, development of clonic seizure, development of tonic-clonic seizures, and severity of seizure were recorded. Additionally, the median severity, percentage of animals that experienced the highest seizure score (stage 5: tonic-clonic seizure), and the percentage mortality for each group was determined. Mean latency ± S.E.M. are presented for each group, together with the median value for seizure severity. Differences in latency and seizure duration values were assessed using one-way analysis of variance (ANOVA) with post-hoc Tukey's test; Mann-Whitney U tests were performed when replicant (n) numbers were insufficient to support post-hoc testing. Differences in seizure incidence and mortality (%) were assessed by a nonparametric binomial test. In all cases, $P \leq 0.05$ was considered to be significant.

Receptor binding assays

Membrane preparation

Cortical tissue was dissected from the brains of adult (P > 21) male and female Wistar Kyoto rats and stored separately at -80°C until use. Tissue was suspended in a membrane buffer, containing (in mM): Tris-HCl 50, $MgCl_2$ 5, EDTA 2 and 0.5 mg/ml fatty acid-free bovine serum albumin (BSA) and Complete protease inhibitor (Roche, Mannheim, Germany), pH 7.4, and was then homogenized using an Ultra-Turrax blender (Labo Moderne, Paris, France). Homogenates were centrifuged at 1000 g at 4°C for 10 min and supernatants decanted and retained. Resulting pellets were re-homogenized and centrifugation was repeated as before. Supernatants were combined and then centrifuged at 39 000 g at 4°C for

30 min in a high-speed Sorvall centrifuge; remaining pellets were resuspended in membrane buffer and protein content determined by the Lowry method (Lowry *et al*., 1951). All procedures were carried out on ice.

Radioligand binding assays

Competition binding assays against the CB_1 receptor antagonist [^{3}H]SR141716A were carried out in triplicate in assay buffer containing (in mM) HEPES 20, EDTA 1, EGTA 1 and 5mg/ml fatty acid-free BSA; pH 7.4. All stock solutions of drugs and membrane preparations were diluted in assay buffer and stored on ice immediately prior to incubation. Assay tubes contained 0.5 nM [^{3}H]SR141716A (K_d = 0.53 ± 0.01 nM, n=3, determined from saturation assay curves) together with drugs at the desired final concentration, and were made up to a final volume of 1 ml with assay buffer. Non-specific binding was determined in the presence of the CB_1 receptor antagonist AM251 (10 μM). Assays were initiated by addition of 50 μg membrane protein. Assay tubes were incubated for 90 min at 25°C and the assay was terminated by rapid filtration through Whatman GF/C filters using a Brandell cell harvester, followed by three washes with ice-cold phosphate buffered saline to remove unbound radioactivity. Filters were incubated overnight in 2 ml scintillation fluid, and radioactivity was quantified by liquid scintillation spectrometry.

[^{35}S]GTPγS binding assays

Assays were carried out in triplicate in assay buffer containing (in mM) HEPES 20, $MgCl_2$ 3, NaCl 60, EGTA 1 and 0.5 mg/ml fatty acid free BSA; pH 7.4. All stock solutions of drugs and membrane preparations were diluted in assay buffer and stored on ice immediately prior

to use. Assay tubes contained guanosine 5'-diphosphate (GDP) at a final concentration of 10 mM, together with drugs at the desired final concentration, and were made up to a final volume of 1 ml with assay buffer. Assays were initiated by addition of 10 μg membrane protein. Assays were incubated for 30 min at 30°C prior to addition of [^{35}S]GTPγS (final concentration 0.1 nM). Assays were terminated after a further 30-min incubation at 30°C by rapid filtration through Whatman GF/C filters using a Brandell cell harvester, followed by three washes with ice-cold phosphate buffered saline to remove unbound radioactivity. Filters were incubated for a minimum of 2 h in 2 ml scintillation fluid, and radioactivity was quantified by liquid scintillation spectrometry.

Data analysis and statistical procedures

Data analyses were performed using GraphPad Prism v4.03 (GraphPad San Diego, CA, USA). Saturation experiments were performed to determine K_d and B_{max} (pmol/mg) values; free radioligand concentration was determined by subtraction of total bound radioligand from the added radioligand concentration. Data for specific radioligand binding and free radioligand concentration were fitted to equations describing one- or two-binding site models, and the best fit determined using an F test. Saturation analyses best fitted a one-binding site model. Competition experiments were fitted to one- and two-binding site models, and the best fit was determined using an F test. Data for the best fits are expressed as K_i values, with the respective percentage of high affinity sites (% R_h) given for two-binding site models (Vivo *et al*., 2006). Hill slope for competition experiments was determined using a sigmoidal concentration–response model (variable slope). [^{35}S]GTPγS concentration–response data were analysed using a sigmoidal concentration–response model (variable

slope) or linear regression and compared using an F-test to select the appropriate model. No other constraints were applied. [^{35}S]GTPγS binding is expressed as percentage increase in radioactivity as previously described (Dennis *et al*., 2008). All data are expressed as mean ± S.E.M.

Pharmacology

The following agents were used: AM251, WIN55,212-2 (Tocris-Cookson, Bristol, UK); CBD (GW Pharmaceuticals, Porton Down, UK); [^{3}H]SR141716A and [^{35}S]GTPγS (GE Healthcare, Chalfont St. Giles, U.K.). All other reagents were from Sigma UK.

Results

Characterisation of Mg^{2+}-free and 4-AP models of epileptiform activity using MEA electrophysiology

In order to investigate neuronal excitability *in vitro*, we used both the Mg^{2+}-free and 4-AP models of epileptiform activity in acute hippocampal brain slices, as measured using MEA electrophysiology. Two separate models of epileptiform activity were used to provide a broader analysis of drug effects (Whalley *et al*., 2009; Hill *et al*., 2009). Hippocampal slices have a well-defined architecture (Fig. 1A), exhibited no spontaneous local field potential (LFP) events in control aCSF and proved readily amenable to MEA recording (Fig. 1B). We sought to take advantage of the ability of MEAs to record spatiotemporal activity at multiple discrete, identifiable regions by investigating activity at CA1, CA3 and DG regions within the hippocampus. Application of Mg^{2+}-free aCSF (Fig. 1C) or 4-AP aCSF (Fig. 1D) to hippocampal slices resulted in the appearance of robust spontaneous epileptiform LFPs across the preparation. LFPs were consistent with *status epilepticus*-like activity and were reliably recorded using the multi-site MEA technique (Table 1). Slice-to-slice variability and electrode contact variability resulted in substantial variation in signal strength (see Table 1); therefore, subsequent drug-induced changes in burst characteristics were normalised to control bursts prior to drug application (these analyses are fully characterised in Hill *et al*., 2009).

Effects of CBD in the Mg^{2+}-free model of in vitro epileptiform activity

We first examined the effects of CBD in the Mg^{2+}-free model to assess CBD effects upon a receptor-dependent model of epileptiform activity. The Mg^{2+}-free model removes the Mg^{2+}-

dependent block of NMDA glutamate receptors rendering them more responsive to synaptically-released glutamate at resting membrane potentials. In Mg^{2+}-free aCSF, CBD significantly decreased LFP burst amplitude in the CA1 (1 – 100 μM CBD) and DG (10 – 100 μM CBD) regions (Fig. 2A,B,Ci). In contrast, CBD (0.01 - 100 μM) effects on LFP burst amplitude in CA3 failed to reach significance. CBD decreased burst duration in CA1 (0.01 - 100 μM CBD), CA3 (0.01 - 100 μM CBD) and DG (0.1 - 100 μM CBD) regions (Fig. 2A,B,Cii). CBD (0.01 - 10 μM) also caused an increase in burst frequency in all regions tested (Fig 2Ciii), but this effect was lost at 100 μM CBD. In order to correlate these data with information on LFP burst initiation and spread across the hippocampal brain slice, we constructed contour plots (Fig. 3A) and associated video animations (Supplemental Fig. 1). Such plots spatiotemporally visualize the '8x8' MEA configuration (Fig. 1B,C) and the individual LFP activity shown in raw data traces (Fig. 2A,B). In these experiments, Mg^{2+}-free aCSF-induced bursts typically originated in the CA3 region of the hippocampal slice preparation and propagated along the principal cell layer towards CA1. LFP events induced by Mg^{2+}-free aCSF had a mean propagation speed of 0.229 ± 0.048 m/s (n=6). CBD (100 μM) caused a clear suppression of Mg^{2+}-free-induced LFP burst amplitude peak source and peak sink values across the hippocampal slice (Fig. 3A; Supplemental Fig. 1). Propagation speed across the brain slice in Mg^{2+}-free aCSF was not affected by 100 μM CBD (0.232 ± 0.076 m/s; n=6; $P > 0.5$). Taken together, these data suggest that, although CBD attenuates epileptiform LFP amplitude and duration in the Mg^{2+}-free model, the rate of signal spread across the preparation is not changed (see Discussion).

Effects of CBD in the 4-AP model of in vitro epileptiform activity

We next examined the effects of CBD upon epileptiform bursting events in the 4-AP model of *status epilepticus*-like activity. 4-AP acts to block postsynaptic voltage-dependent K^+ channels and inhibits neuronal repolarisation to effectively increase excitability. In 100 μM 4-AP aCSF, CBD (100 μM) caused a significant decrease in LFP burst amplitude in CA1 only (Fig. 4A,B,Ci). In contrast, CBD (0.01 – 0.1 μM) caused an unexpected small, but significant increase in LFP burst amplitude in DG, which was not apparent at higher CBD concentrations in this, or other, hippocampal regions (Fig. 4Ci). CBD caused a decrease in burst duration in DG (0.01 – 100 μM CBD), CA3 (0.1 – 100 μM CBD), but was without overall effect on CA1 (Fig. 4A,B,Cii). CBD (0.01 - 100 μM) also caused a significant decrease in burst frequency in all regions tested (Fig. 4Ciii). In the same manner as for the Mg^{2+}-free model, contour plots of 4-AP-induced epileptiform LFP burst events (Fig. 3B) permitted spatiotemporal visualization of activity across the slice preparation (Supplemental Fig. 1). 4-AP aCSF-induced bursts typically initiated in CA3 before spreading to CA1 with a propagation speed of 0.146 ± 0.033 m/s (n=5). CBD (100 μM) caused a clear suppression of 4-AP-induced epileptiform LFP burst amplitude (Fig. 3B; Supplemental Fig. 1). Propagation speed across the brain slice in 4-AP aCSF was not affected by 100 μM CBD (0.176 ± 0.046 m/s, n=6; $P > 0.5$).

Taken together, these data show that CBD displayed clear concentration-related, region-specific, anticonvulsant properties in two different *in vitro* models of epileptiform activity, attenuating LFP burst amplitude and duration, but with no effect on the rate of signal propagation in either model.

Effects of CBD in the pentylenetetrazole (PTZ) model of generalised seizures.

We next assessed the effects of CBD (1, 10 and 100 mg/kg; ip) on PTZ-induced generalised seizures in adult male rats. PTZ acts as a $GABA_A$ receptor antagonist and this model is well-defined and standardly used for the identification of potential anticonvulsants to treat generalised clonic seizures (Loscher *et al*., 1991). Seizures were defined by a standard scoring scale (see Materials and Methods). CBD at any dose did not significantly alter the latency to first sign of PTZ-induced seizures (Fig. 5A) or latency to development of clonic (Fig. 5B) seizures. Unexpectedly, CBD (1 mg/kg) reduced latency to tonic-clonic seizures (Fig. 5C, $P<0.01$). No other effects of CBD on latency to specific seizure states were observed. In contrast to the lack of definitive effects on seizure latency, CBD (100 mg/kg) demonstrated clear anticonvulsant effects via measures of seizure severity (Fig. 6A,B) and mortality (Fig. 6C). When considering the severity of PTZ-induced seizures, vehicle-treated animals reached a median score of 5 (tonic-clonic seizures with a loss of righting reflex), the most severe on the scoring scale (Fig. 6A). In contrast, animals treated with 100 mg/kg CBD exhibited a significantly reduced median score of 3.5 (forelimb clonus with tonic component, but with righting reflex preserved; Fig. 6A, n=15 animals; $P<0.001$). This was associated with a marked decrease in the proportion of animals that developed the most severe tonic-clonic seizures, which was reduced from 53% in vehicle to 7% by 100 mg/kg CBD (n=15 animals, $P<0.001$; Fig. 6B). Finally, percentage mortality was significantly reduced from 47% in vehicle to 7% by 100 mg/kg CBD (n=15 animals, $P<0.001$; Fig. 6C). Overall, these *in vivo* data confirm our *in vitro* results above and fully support an anticonvulsant action for CBD.

Effects of CBD in receptor binding assays

JPET Fast Forward. Published on November 11, 2009 as DOI: 10.1124/jpet.109.159145
This article has not been copyedited and formatted. The final version may differ from this version.

It is known that hippocampal CB_1 receptor expression on glutamatergic terminals is selectively down-regulated under epileptic conditions (Ludanyi *et al*., 2008); moreover, activation of CB_1 receptors by eCBs is protective against seizures (Monory *et al*., 2006) and exogenous CB_1 agonists decrease epileptiform activity in hippocampal neurons (Blair *et al*., 2006; Shen & Thayer, 1999). Therefore, we determined potential CBD actions at CB_1 receptors. Competition binding assays were performed for CBD against the CB_1 receptor antagonist [^{3}H]SR141716A in isolated cortical membranes; CBD effects were compared with those of the standard synthetic CB receptor agonist WIN55,212-2 and the CB_1 receptor antagonist AM251 (Fig. 7A). AM251 displacement of [^{3}H]SR141716A binding occurred with high affinity (K_i = 190 ± 56 pM; n= 4) and was best fitted by a one-site competition model (Hill slope = -1.08 ± 0.13; n=4). In contrast, WIN55,212-2 displacement was best fitted to a two-site model with a high (K_i = 7.03 ± 4.1 nM; % R_h = 27.4 ± 5.0%; n =4) and a low (K_i = 904 ± 155 nM; n=4) affinity site; in these experiments, Hill slopes for either the low or high affinity site did not match unity. CBD displacement of [^{3}H]SR141716A occurred with low affinity (K_i = 1.82 ± 0.38 μM; n= 4) and was best fitted by a one-site model (Hill slope = -1.15 ± 0.11; n=4).

Finally, we investigated potential functional effects of CBD using [^{35}S]GTPγS binding assays in rat cortical membranes; CBD actions were compared with effects of WIN55,212-2 and AM251 (Fig. 7B). We first confirmed the presence of functional CB receptors. Accordingly, WIN55,212-2 caused an increase in percentage stimulation of [^{35}S]GTPγS binding with an EC_{50} of 95.1 ± 0.1 nM (n=3); for 10 μM WIN55,212-2, E_{max} = 98.6 ± 3.5% (*n* = 3). AM251 had no stimulatory effect on [^{35}S]GTPγS binding at tested concentration <1 μM; at micromolar concentrations AM251 caused a moderate depression of

JPET Fast Forward. Published on November 11, 2009 as DOI: 10.1124/jpet.109.159145
This article has not been copyedited and formatted. The final version may differ from this version.

[^{35}S]GTPγS binding (10 μM AM251: -20.3 ± 4.3%, n=3). CBD had no effect at concentrations ≤ 1 μM; large decreases in [^{35}S]GTPγS binding were seen at 10 μM CBD (-28.8 ± 10.3%, n=3) and 100 μM CBD (-76.7 ± 15.9% , n=3).

Thus, overall, CBD had clear anti-epileptogenic and anti-seizure effects, but only low affinity and no clear agonist effects at cortical CB_1 receptors.

Discussion

CBD reduces excitability in in vitro models of epileptiform activity

In the present study, we use extracellular MEA recordings to demonstrate that CBD attenuates epileptiform activity in both the Mg^{2+}-free and 4-AP *in vitro* models of *status epilepticus* in the mammalian hippocampus, a prominent epileptogenic region (Ben-Ari and Cossart, 2000). The major effects of CBD were to decrease LFP burst amplitude and duration in a hippocampal region-specific manner. In general, the CA1 region was most sensitive to CBD effects. Thus, LFP amplitude was significantly reduced at lower CBD concentrations in CA1 than CA3 (with DG remaining unaffected) in Mg^{2+}-free aCSF and CA1 was the only region in which LFP amplitude was affected in 4-AP aCSF. This is of interest as the CA1 region represents the major output of the hippocampus, relaying information to cortical and subcortical sites and is intimately involved in propagation of epileptic activity (McCormick and Contreras, 2001). Contour plots constructed from data in the Mg^{2+}-free and 4-AP models confirmed that LFP bursts typically originated in the CA3 region and propagated towards CA1 (see Feng and Durand, 2004), strongly suggesting that CA1 is a major focus of epileptic activity in the two models used and illustrated that CBD exerts a significant anti-epileptiform effect in this region.

Overall, CBD induced more prominent effects in Mg^{2+}-free than in 4-AP aCSF. This may reflect inherent differences between the two models, which affect NMDA glutamate receptors and K^+ channels, respectively. CBD had contrasting actions on LFP burst frequency between models, frequency was increased in all regions by CBD in Mg^{2+}-free aCSF, but was decreased in all regions in 4-AP aCSF. Interestingly, 100 μM CBD was without effect on burst frequency in the Mg^{2+}-free model, in contrast to data for all the lower

concentrations of CBD tested. This finding was the only indication of any biphasic action of CBD, a common phenomenon associated with cannabinoids whereby increasing concentrations cause changes in the pharmacological 'direction' of action (Pertwee, 2008).

In light of the region-specific effects of CBD, it will be of interest in the future to investigate the cellular mechanisms of action of CBD using intracellular recording from individual neurons in selected hippocampal regions. In both the Mg^{2+}-free and 4-AP models, contour plots and subsequent analyses showed that CBD caused clear attenuation in LFP burst amplitude, but had no overall effect on burst propagation speed. These findings suggest that CBD acts to reduce the magnitude of epileptiform activity whilst leaving speed of information transmission across the hippocampal slice intact. Interestingly, it is possible that this may result in a more tolerable side-effect profile for CBD in comparison to existing AEDs if used in a clinical setting.

CBD has anticonvulsant properties in the PTZ model of generalised seizures

CBD had beneficial effects on seizure severity and lethality in response to PTZ administration without delaying the time taken for seizures to develop. CBD (100 mg/kg) demonstrated clear anticonvulsant effects in terms of significant reductions in median seizure severity, tonic-clonic seizures and mortality. Particularly striking effects were that <10% of animals developed tonic-clonic seizures or suffered mortality when treated with CBD in comparison to around 50% of vehicle-treated animals. The present data strongly substantiate a number of earlier *in vivo* studies suggesting that CBD has anticonvulsant potential (Lutz, 2004; Scuderi *et al*., 2009). CBD has been reported to have a relatively potent anticonvulsant action in maximal electroshock (a model of partial seizure with secondary generalization) (Karler *et al*., 1974; Consroe and Wolkin,

1977). Moreover, CBD prevented tonic-clonic seizures in response to electroshock current (Consroe *et al.*, 1982). There is limited clinical data on CBD effects on seizure frequency in humans (Gordon and Devinsky, 2001). However, in one small double-blind study, of 8 patients with uncontrolled secondary generalised epilepsy treated with 200-300 mg CBD, 4 remained symptom-free and 3 had signs of improvement (Cunha *et al*., 1980). One potential concern was the high doses of CBD used by Cunha *et al*. (1980). As all new therapies must be introduced initially in an adjunct capacity to existing medication, the present study suggests that one attractive possibility is a role for CBD as an adjunct in generalised seizures. In this regard, earlier animal studies indicate that CBD enhances the effects of phenytoin (although CBD reduced the potency of other AEDs) (Consroe and Wolkin, 1977). In the future, it will be of interest to extend studies to other animal seizure models and also to combination therapies with selective AEDs to determine the full clinical anticonvulsant potential of CBD against a range of epilepsy phenotypes.

Mechanism of action

Cannabinoid actions are mediated by CB_1 and CB_2 receptors, potentially by the GPR55 receptor, but also by cannabinoid receptor-independent mechanisms (Howlett *et al*., 2004; Ryberg *et al*., 2007). In regard to epilepsy, CB_1 receptors are densely expressed in the hippocampal formation (Herkenham *et al*. 1990; Tsou et al. 1999) where their activation is widely reported to be anti-epileptic in animal models (Shen and Thayer, 1999; Wallace *et al*., 2001; but see Clements *et al*., 2003). Here, we demonstrate that CBD displaced the selective CB_1 receptor antagonist [^{3}H]SR141716A in cortical membranes with relatively low affinity (K_i = 1.82 μM); these data are in line with values reported in whole brain membranes (reviewed in Pertwee, 2008) and our

data in cerebellar membranes (Smith *et al*., 2009). CB receptor/G-protein coupling may differ between distinct brain regions (Breivogel *et al*., 1997; Dennis *et al*., 2008); therefore, we investigated CBD effects on [^{35}S]GTPγS binding in isolated cortical membranes. We show that CBD has no stimulatory agonist activity, but that CBD at micromolar concentrations decreases G protein activity. These findings are also in agreement with studies in mouse whole brain membranes (Thomas *et al*. 2007) who report that CBD has only low affinity at CB_1 and CB_2 receptors, but acts efficaciously as an antagonist at both receptor types (Thomas *et al*., 2007; see Pertwee, 2008). There are a number of potential mechanisms by which ligands acting at CB receptors may mediate anticonvulsant effects. Receptor agonists may act at CB_1 on excitatory presynaptic terminals to inhibit glutamate neurotransmitter release. Such a mechanism is unlikely here as CBD has no agonist effect in GTPγS binding assays (see also Thomas *et al*., 2007). An alternative is that antagonists act at CB_1 receptors on inhibitory presynaptic terminals to increase GABA release. We have demonstrated such a mechanism for the phytocannabinoid Δ^9-THCV in the cerebellum (Ma *et al*., 2008), where displacement of eCB tone may lead to increased inhibition. It may also be speculated that the decreases in G protein activity seen in GTPγS binding assays represent an inverse agonist action at CB_1 receptors; for example, if CBD were acting as an inverse agonist at CB_1 receptors on inhibitory presynaptic terminals an increase in GABA release could lead to reduced excitability. However, mechanisms involving increases in GABA release are unlikely here as CBD was effective in reducing seizures *in vivo* in the presence of the $GABA_A$ receptor antagonist PTZ. Moreover, CBD-induced reductions in [^{35}S]GTPγS binding to whole brain membranes were retained in CB_1 knock-out (*cnr1*-/-) mice suggesting that CBD is not an inverse agonist at CB_1 receptors (Thomas *et al*., 2007). Overall, the low affinity and lack of agonist activity at CB_1 receptors suggests that CBD anticonvulsant

effects reported here are most likely mediated by CB_1 receptor-independent mechanisms. In addition to the study of Thomas *et al*, showing CBD actions were unaltered in *cnr1*-/- mice, CBD anticonvulsant effects in the maximal electroshock model were unaffected by the CB_1 receptor antagonist SR141716A, whereas those of Δ^9-THC and WIN55,212-2 were blocked (Wallace *et al*., 2001).

In addition to CB receptors, a number of alternative molecular targets may also contribute to CBD effects on neuronal excitability. CBD has been reported to be an antagonist at GPR55, a non-CB_1/CB_2 receptor (Ryberg *et al*., 2007); in contrast, a recent study demonstrates that CBD has no effect at GPR55 (Kapur *et al*., 2009). CBD may cause an increase in anticonvulsant eCBs via the reported inhibition of the catabolic enzyme fatty acid hydrolyase, which degrades anandamide, and/or the blockade of anandamide uptake (Rakhshan *et al*., 2000; Watanabe *et al*., 1996; Bisogno *et al*., 2001). CBD is reported to be a weak agonist at human TRPV1 receptors (Bisogno *et al*., 2001); a more recent study suggests an action for CBD at rat and human TRPV2, but not rat TRPV1, receptors (Qin *et al*., 2008). More relevant to potential effects on neuronal excitability in the CNS is the demonstration that CBD exerts a bidirectional action on $[Ca^{2+}]_i$ levels in hippocampal neurons (Ryan *et al*., 2009). Under control conditions, CBD induces increases in $[Ca^{2+}]_i$; in contrast, in the presence of 4-AP (which induces seizure-like $[Ca^{2+}]_i$ oscillations) or increased extracellular K^+, CBD acts to reduce $[Ca^{2+}]_i$, and thus epileptiform activity, via an action on mitochondria Ca^{2+} stores. A further recent report provides the first evidence that CBD can also block low-voltage-activated (T-type) Ca^{2+} channels (Ross *et al*., 2008), important modulators of neuronal excitability. Finally, CBD may also enhance the activity of inhibitory glycine receptors (Ahrens *et al*., 2009). Overall, the demonstration that

CBD acts on multiple molecular targets that each play a key role in neuronal excitability reinforces the potential of CBD as an AED.

Conclusions

Our data in separate *in vitro* models of epileptiform activity and, in particular, the beneficial reductions in seizure severity caused by CBD in an *in vivo* animal model of generalised seizures suggests that earlier, small-scale clinical trials for CBD in untreated epilepsy warrant urgent renewed investigation.

Acknowledgements

We would like to thank Professor Philip Strange for useful discussion and Colin Stott (GW Pharmaceuticals) and Professor Gernot Riedel (University of Aberdeen) for pharmacokinetics data.

References

Abramoff MD, Magelhaes PJ, and Ram SJ (2004) Image Processing with ImageJ. *Biophotonics International* **11**:36-42.

Ahrens J, Demir R, Leuwer M, de la Roche J, Krampfl K, Foadi N, Karst M, and Haeseler G (2009) The nonpsychotropic cannabinoid cannabidiol modulates and directly activates α1 and α1β glycine receptor function. *Pharmacology* **83**:217-222.

Bisogno T, Hanus L, De Petrocellis L, Tchilibon S, Ponde DE, Brandi I, Moriello AS, Davis JB, Mechoulam R, and Di Marzo V (2001) Molecular targets for cannabidiol and its synthetic analogues: effect on vanilloid VR1 receptors and on the cellular uptake and enzymatic hydrolysis of anandamide. *Br J Pharmacol* **134**:845-852.

Ben-Ari Y and Cossart R (2001) Kainate, a double agent that generates seizures: two decades of progress. *Trends Neurosci* **23**:580-587.

Bhattacharyya S, Fusar-Poli P, Borgwardt S, Martin-Santos R, Nosarti C, O'Carroll C, Allen P, Seal ML, Fletcher PC, Crippa JA, Giampietro V, Mechelli A, Atakan Z, and McGuire P (2009) Modulation of mediotemporal and ventrostriatal function in humans by Δ^9-tetrahydrocannabinol: a neural basis for the effects of *Cannabis sativa* on learning and psychosis. *Arch Gen Psychiatry* **66**:442-451.

Blair RE, Deshpande LS, Sombati S, Falenski KW, Martin BR, and DeLorenzo RJ (2006) Activation of the cannabinoid type-1 receptor mediates the anticonvulsant properties of cannabinoids in the hippocampal neuronal culture models of acquired epilepsy and status epilepticus. *J Pharmacol Exp Ther* **317**:1072-1078.

Breivogel CS, Sim LJ, and Childers SR (1997) Regional differences in cannabinoid receptor/G-protein coupling in rat brain. *J Pharmacol Exp Ther* **282**:1632-1642.

Clement AB, Hawkins EG, Lichtman AH, and Cravatt BF (2003) Increased seizure susceptibility and proconvulsant activity of anandamide in mice lacking fatty acid amide hydrolase. *J Neurosci* **23**:3916-3923.

Consroe P and Wolkin A (1977) Cannabidiol-antiepileptic drug comparisons and interactions in experimentally induced seizures in rats. *J Pharmacol Exp Ther* **201**:26-32.

Consroe P, Benedito MA, Leite JR, Carlini EA, and Mechoulam R (1982) Effects of cannabidiol on behavioral seizures caused by convulsant drugs or current in mice. *Eur J Pharmacol* **83**:293-298.

Cunha JM, Carlini EA, Pereira AE, Ramos OL, Pimentel C, Gagliardi R, Sanvito WL, Lander N, and Mechoulam R (1980) Chronic administration of cannabidiol to healthy volunteers and epileptic patients. *Pharmacology* **21**:175-185.

Dennis I, Whalley BJ, and Stephens GJ (2008) Effects of Δ^9-tetrahydrocannabivarin on [^{35}S]GTPγS binding in mouse brain cerebellum and piriform cortex membranes. *Br J Pharmacol* **154**:1349-1358.

Egert U, Heck D, and Aertsen A (2002a) Two-dimensional monitoring of spiking networks in acute brain slices. *Exp Brain Res* **142**:268-274.

Egert U, Knott T, Schwarz C, Nawrot M, Brandt A, Rotter S, and Diesmann M (2002b) MEA-Tools: an open source toolbox for the analysis of multi-electrode data with MATLAB. *J Neurosci Methods* **117**:33-42.

Farrimond JA, Hill AJ, Jones NA, Stephens GJ, Whalley BJ, and Williams CM (2009) A cost-effective high-throughput digital system for observation and acquisition of animal behavioral data. *Behav Res Methods* **41**:446-451.

Feng Z, and Durand DM (2005) Decrease in synaptic transmission can reverse the propagation direction of epileptiform activity in hippocampus *in vivo. J Neurophysiol* **93**:1158-1164.

Gordon E and Devinsky O (2001) Alcohol and marijuana: effects on epilepsy and use by patients with epilepsy. *Epilepsia* **42**:1266-12672.

Hampson AJ, Grimaldi M, Axelrod J, and Wink D (1998) Cannabidiol and (-)Δ^9-tetrahydrocannabinol are neuroprotective antioxidants. *Proc Natl Acad Sci USA* **95**:8268-8273.

Herkenham M, Lynn AB, Little MD, Johnson MR, Melvin LS, de Costa BR, and Rice KC (1990) Cannabinoid receptor localization in brain. *Proc Natl Acad Sci USA* **87**:1932-1936.

Hill AJ, Jones NA, Williams CM, Stephens GJ, and Whalley BJ (2009) Development of multi-electrode array screening for anticonvulsants in acute rat brain slices. *J Neurosci Methods* Oct 13 [Epub ahead of print]

Howlett AC, Breivogel CS, Childers SR, Deadwyler SA, Hampson RE, and Porrino LJ (2004) Cannabinoid physiology and pharmacology: 30 years of progress. *Neuropharmacol* **47**:345–358.

Iuvone T, Esposito G, De Filippis D, Scuderi C, and Steardo L (2009) Cannabidiol: a promising drug for neurodegenerative disorders? *CNS Neurosci Ther* **15**:65-75.

Kapur A, Zhao P, Sharir H, Bai Y, Caron MG, Barak LS, Abood ME. Atypical responsiveness of the orphan receptor GPR55 to cannabinoid ligands. J Biol Chem. 2009 Sep 1. [Epub ahead of print]

Karler R, Cely W, and Turkanis SA (1974) Anticonvulsant properties of Δ^9-tetrahydrocannabinol and other cannabinoids. *Life Sci* **15**:931-947.

Kwan P and Brodie MJ (2007) Emerging drugs for epilepsy. *Expert Opin Emerg Drugs* **12**:407-422.

Löscher W, Hönack D, Fassbender CP, and Nolting B (1991) The role of technical, biological and pharmacological factors in the laboratory evaluation of anticonvulsant drugs. III. Pentylenetetrazole seizure models. *Epilepsy Res* **8**:171-189.

Lowry OH, Rosebrough NJ, Farr AL, and Randall RJ (1951) Protein measurement with the folin phenol reagent. *J Biol Chem* **193**:265-275.

Ludányi A, Eross L, Czirják S, Vajda J, Halász P, Watanabe M, Palkovits M, Maglóczky Z, Freund TF, and Katona I (2008) Downregulation of the CB_1 cannabinoid receptor and related molecular elements of the endocannabinoid system in epileptic human hippocampus. *J Neurosci* **28:**2976-2990.

Lutz, B (2004) On-demand activation of the endocannabinoid system in the control of neuronal excitability and epileptiform seizures. *Biochem Pharmacol* **68:**1691-1698.

Ma YL, Weston SE, Whalley BJ, and Stephens GJ (2008) The phytocannabinoid Δ^9-tetrahydrocannabivarin modulates inhibitory neurotransmission in the cerebellum. *Br J Pharmacol* **154**:204-215.

McCormick DA and Contreras D (2001) On the cellular and network bases of epileptic seizures. *Annu Rev Physiol* **63**:815-846.

Mechoulam R and Shvo Y (1963) Hashish. I. The structure of cannabidiol. *Tetrahedron* **19**:2073-2078.

Monory K, Massa F, Egertová M, Eder M, Blaudzun H, Westenbroek R, Kelsch W, Jacob W, Marsch R, Ekker M, Long J, Rubenstein JL, Goebbels S, Nave KA, During M, Klugmann M, Wölfel B, Dodt HU, Zieglgänsberger W, Wotjak CT, Mackie K, Elphick MR, Marsicano G, and Lutz B (2006) The endocannabinoid system controls key epileptogenic circuits in the hippocampus. *Neuron* **51**:455-466.

Pohl M and Mares P (1987) Effects of flunarizine on Metrazol-induced seizures in developing rats. *Epilepsy Res* **1**:302-305.

Pertwee RG (2008) The diverse CB_1 and CB_2 receptor pharmacology of three plant cannabinoids: Δ^9-tetrahydrocannabinol, cannabidiol and Δ^9-tetrahydrocannabivarin. *Br J Pharmacol* **153:**199-215.

Qin N, Neeper MP, Liu Y, Hutchinson TL, Lubin ML, and Flores CM (2008) TRPV2 is activated by cannabidiol and mediates CGRP release in cultured rat dorsal root ganglion neurons. *J Neurosci* **28**:6231-6238.

Rakhshan F, Day TA, Blakely RD, and Barker EL (2000) Carrier-mediated uptake of the endogenous cannabinoid anandamide in RBL-2H3 cells. *J Pharmacol Exp Ther* **292**:960–967.

Ross HR, Napier I, and Connor M (2008) Inhibition of recombinant human T-type calcium channels by Δ^9-tetrahydrocannabinol and cannabidiol. *J Biol Chem* **283**:16124-16134.

Ryan D, Drysdale AJ, Lafourcade C, Pertwee RG, and Platt B. (2009) Cannabidiol targets mitochondria to regulate intracellular Ca^{2+} levels. *J Neurosci* **29**:2053-2063.

Ryberg E, Larsson N, Sjögren S, Hjorth S, Hermansson NO, Leonova J, Elebring T, Nilsson K, Drmota T, and Greasley PJ (2007) The orphan receptor GPR55 is a novel cannabinoid receptor. *Br J Pharmacol* **152**:1092-1101.

Sagredo O, Ramos JA, Decio A, Mechoulam R, and Fernández-Ruiz J (2007) Cannabidiol reduced the striatal atrophy caused 3-nitropropionic acid *in vivo* by mechanisms independent of the activation of cannabinoid, vanilloid TRPV1 and adenosine A2A receptors. *Eur J Neurosci* **26**:843-851.

Scuderi C, Filippis DD, Iuvone T, Blasio A, Steardo A, and Esposito G (2009) Cannabidiol in medicine: a review of its therapeutic potential in CNS disorders. *Phytother Res* **23**:597-602.

Shen M and Thayer SA (1999) Δ^9-tetrahydrocannabinol acts as a partial agonist to modulate glutamatergic synaptic transmission between rat hippocampal neurons in culture. *Mol Pharmacol* **55**:8–13.

Smith I, Bevan SA, Whalley BJ, and Stephens GJ (2009) Phytocannabinoid affinities at CB_1 receptors in the mouse cerebellum. International Cannabinoid Research Society 19th Annual Meeting, Pheasant Run, Illinois, USA; abstract.

Stett A, Egert U, Guenther E, Hofmann F, Meyer T, Nisch W, and Haemmerle H (2003) Biological application of microelectrode arrays in drug discovery and basic research. *Anal Bioanal Chem* **377**:486-495.

Straiker A and Mackie K (2005) Depolarization-induced suppression of excitation in murine autaptic hippocampal neurones. *J Physiol* **569**:501-517.

Thomas A, Baillie G, Philips AM, Razdan RK, Ross RA, and Pertwee RG (2007) Cannabidiol displays unexpectedly high potency as an antagonist of CB_1 and CB_2 receptor agonists *in vitro*. *Br J Pharmacol* **150**:917-926.

Tsou K, Brown S, Sanudo-Pena MC, Mackie K, and Walker JM (1998) Immunohistochemical distribution of cannabinoid CB_1 receptors in the rat central nervous system. *Neurosci* **83**:393-411.

Vivo M, Lin H, and Strange PG (2006) Investigation of cooperativity in the binding of ligands to the D_2 dopamine receptor. *Mol Pharmacol* **69**:226-235.

Wallace MJ, Wiley JL, Martin BR, and DeLorenzo RJ (2001) Assessment of the role of CB_1 receptors in cannabinoid anticonvulsant effects. *Eur J Pharmacol* **428**:51-57.

Wallace MJ, Martin BR, and DeLorenzo RJ (2002) Evidence for a physiological role of endocannabinoids in the modulation of seizure threshold and severity. *Eur J Pharmacol* **452**:295-301.

Watanabe K, Kayano Y, Matsunaga T, Yamamoto I, and Yoshimura H (1996) Inhibition of anandamide amidase activity in mouse brain microsomes by cannabinoids. *Biol Pharm Bull* **19**:1109–1111.

Whalley BJ, Stephens GJ and Constanti A (2009) Investigation of the effects of the novel anticonvulsant compound carisbamate (RWJ-333369) on rat piriform cortical neurones *in vitro*. *Br J Pharmacol* **156**:994-1008

Footnotes

This work was supported by a GW Pharmaceuticals and Otsuka Pharmaceuticals award to NJ, AH, CMW, BJW and GJS and a University of Reading Research Endowment Trust Fund award to IS. Part of this work was supported by The Wellcome Trust to GJS [Ref: 070739].

Legends for figures

Figure 1. Hippocampal slices are amenable to MEA recording.

A) Schematic representation of hippocampal slice showing position of CA1, CA3 and DG regions, together with major pathways: Schaffer collateral (sc), mossy fibre (mf) and perforant pathway (pp). B) Micrograph showing a hippocampal brain slice (stained with pontamine blue) mounted onto a substrate-integrated MEA (60 electrodes of 30 μm diameter, spaced 200 μm apart in an ~8x8 arrangement). Scale bar = 400 μm. Representative LFP burst activity recorded at 60 electrodes across a hippocampal slice in (C) Mg^{2+}-free aCSF and (D) 4-AP aCSF. Traces were high passed filtered in MC_rack at 2 Hz.

Figure 2. CBD attenuates epileptiform activity induced by Mg^{2+}-free aCSF.

A) Representative traces showing effects of 100 μM CBD on Mg^{2+}-free aCSF-induced LFP bursts in different regions of hippocampal slice. Dotted lines represent an individual LFP (as shown in B). B) Effects of 1 and 100 μM CBD on a representative individual Mg^{2+}-free aCSF-induced LFP burst. C) Bar graphs showing the effects of acute treatment of increasing CBD concentrations upon (i) normalised burst amplitude, (ii) normalised burst duration and (iii) normalised burst frequency in Mg^{2+}-free aCSF. Note that burst amplitudes have been adjusted for run-down and burst frequencies have been adjusted for run-up as described in Material and Methods. Values are mean ± S.E.M for the last 10 LFP bursts in each condition; * = $P \leq 0.05$; ** = $P \leq 0.01$; *** = $P \leq 0.001$ (two-tailed Mann-Whitney U-test).

Figure 3. CBD attenuates epileptiform activity induced by Mg^{2+}-free and 4-AP aCSF.

Representative contour plots illustrating CBD effects upon spatiotemporal epileptiform burst features. (A) In the continued presence of Mg^{2+}-free aCSF: (i) quiescent period between epileptiform burst events also showing hippocampal slice orientation, (ii) peak source in the absence of CBD and (iii) peak source in the presence of CBD (100 μM). (B) In the continued presence of 100 μM 4-AP: (i) quiescent period between epileptiform burst events also showing hippocampal slice orientation, (ii) peak source in the absence of CBD and (iii) peak source in the presence of CBD (100 μM).

Figure 4. CBD attenuates epileptiform activity induced by 4-AP aCSF.

A) Representative traces showing effects of 100 μM CBD on 4-AP aCSF-induced LFP bursts in different regions of hippocampal slice. Dotted lines represent an individual LFP (as shown in B). B) Effects of 1 and 100 μM CBD on a representative individual 4-AP aCSF-induced LFP burst. C) Bar graphs showing the effects of acute treatment of increasing CBD concentrations upon (i) normalised burst amplitude, (ii) normalised burst duration and (iii) normalised burst frequency in the 4-AP aCSF. Note that burst amplitudes have been adjusted for run-down and burst frequencies have been adjusted for run-up as described in Material and Methods. Values are mean ± S.E.M for the last 10 LFP bursts in each condition; * = $P \leq 0.05$; ** = $P \leq 0.01$; *** = $P \leq 0.001$ (two-tailed Mann-Whitney U-test).

Figure 5. CBD has no clear effects on seizure latency *in vivo*.

Bar graphs showing lack of effects of CBD (1, 10 and 100 mg/kg) on A) latency to first sign of seizure; B) latency to clonic seizures and C) latency to tonic-clonic seizures. Each data set n=15 animals. NB. CBD (1 mg/kg) reduced latency to tonic-clonic seizures, this *pro-*

convulsant action was not observed at higher CBD doses; ** = P≤0.01 (one-way analysis of variance (ANOVA) with post-hoc Tukey's test).

Figure 6. CBD reduces seizure severity and mortality *in vivo*.

Bar graphs showing effects of CBD (1, 10 and 100 mg/kg) on A) median seizure severity; B) percentage of animals reaching tonic-clonic seizures and C) percentage mortality. Each data set n=15 animals. CBD (100 mg/kg) significantly reduced all of these parameters; *** = P≤0.001 (nonparametric binomial test).

Figure 7. CBD displaces [^{3}H]SR141716A binding with low affinity and lacks agonist effects in [^{35}S]GTPγS binding assays in cortical membranes.

A) Representative competition curves for the CB receptor agonist WIN55,212-2, the selective CB_1 receptor antagonist AM251 and CBD against 1 nM [3H]SR141716A (a selective CB_1 receptor antagonist) binding to cortical membranes. Points are mean ± S.E.M. of triplicate points. B) Agonist binding curves for the CB receptor agonist WIN55,212-2, the selective CB_1 receptor antagonist AM251 and CBD stimulation of [^{35}S]GTPγS binding to cortical membranes. Points are mean ± S.E.M. of triplicate points from 3 separate experiments.

JPET Fast Forward. Published on November 11, 2009 as DOI: 10.1124/jpet.109.159145
This article has not been copyedited and formatted. The final version may differ from this version.

Table 1. Characterisation measures for the Mg^{2+}-free- and 4-AP- (100 µM) aCSF induced LFP epileptiform activity in the CA1, CA3 and DG regions of the hippocampus.

***In vitro* model**	**Hippocampal region**	**LFP peak burst amplitude (µV)**			**Mean ± S.E.M LFP burst duration (ms)**	**Mean ± S.E.M LFP burst frequency (Hz)**
		Minimum	**Maximum**	**Mean ± S.E.M**		
Mg^{2+} -free	CA1 (n=15)	77	438	257 ± 30	747 ± 29	0.31 ± 0.01
	CA3 (n=12)	37	971	303 ± 88	722 ± 31	0.30 ± 0.02
	DG (n=15)	66	781	275 ± 53	715 ± 28	0.30 ± 0.02
4-AP (100 µM)	CA1 (n=15)	54	383	201 ± 26	508 ± 21	0.77 ± 0.08
	CA3 (n=13)	13	1218	364 ± 101	524 ± 19	0.71 ± 0.07
	DG (n=18)	44	674	338 ± 44	552 ± 12	0.75 ± 0.06

LFP peak burst amplitude values are presented as a minimum and maximum range and mean ± S.E.M. LFP burst duration and frequencies are represented as mean ± S.E.M. A minimum of six separate hippocampal slices were used in the characterisation of each *in vitro* model.

Figure 1

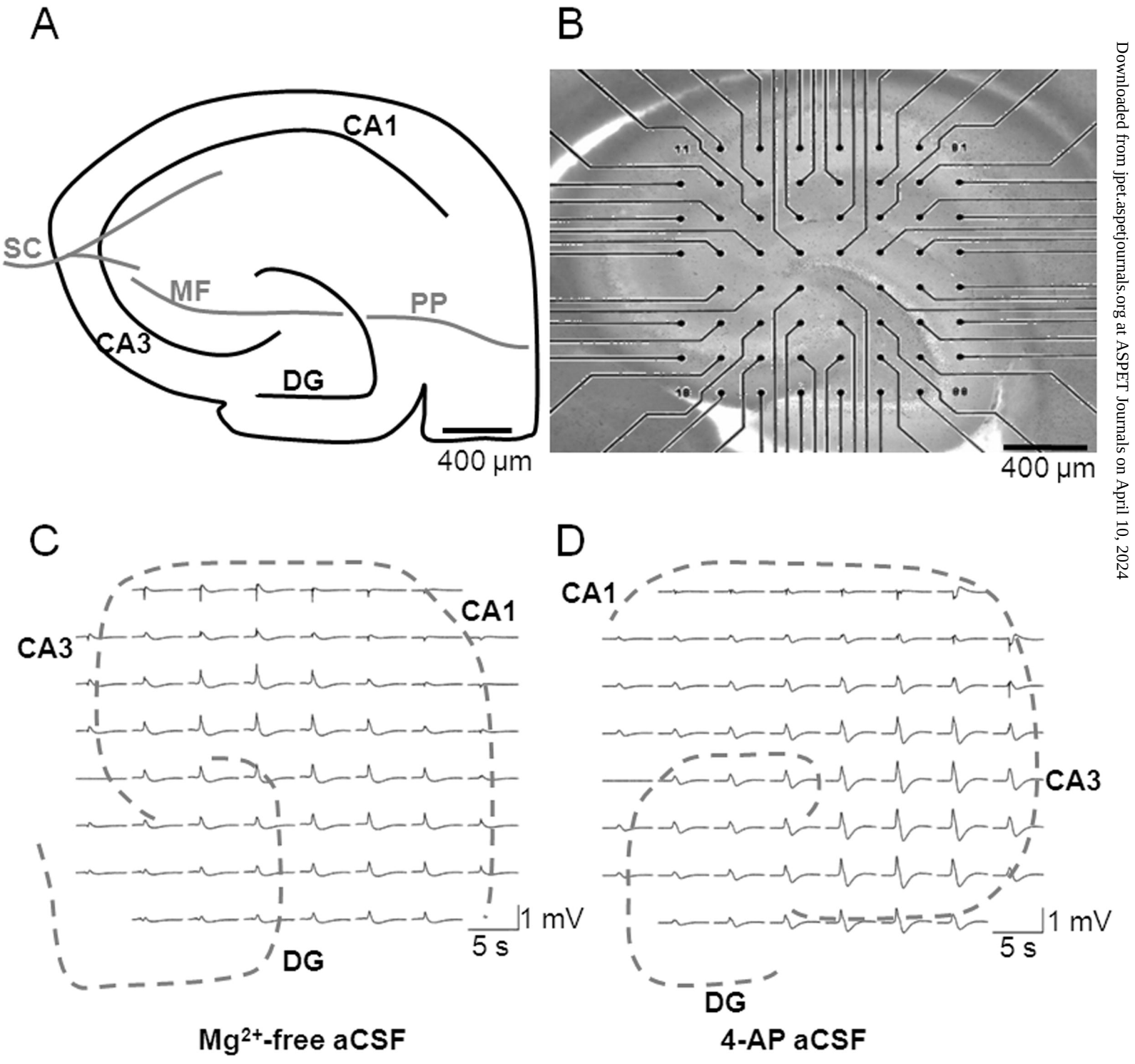

Figure 2

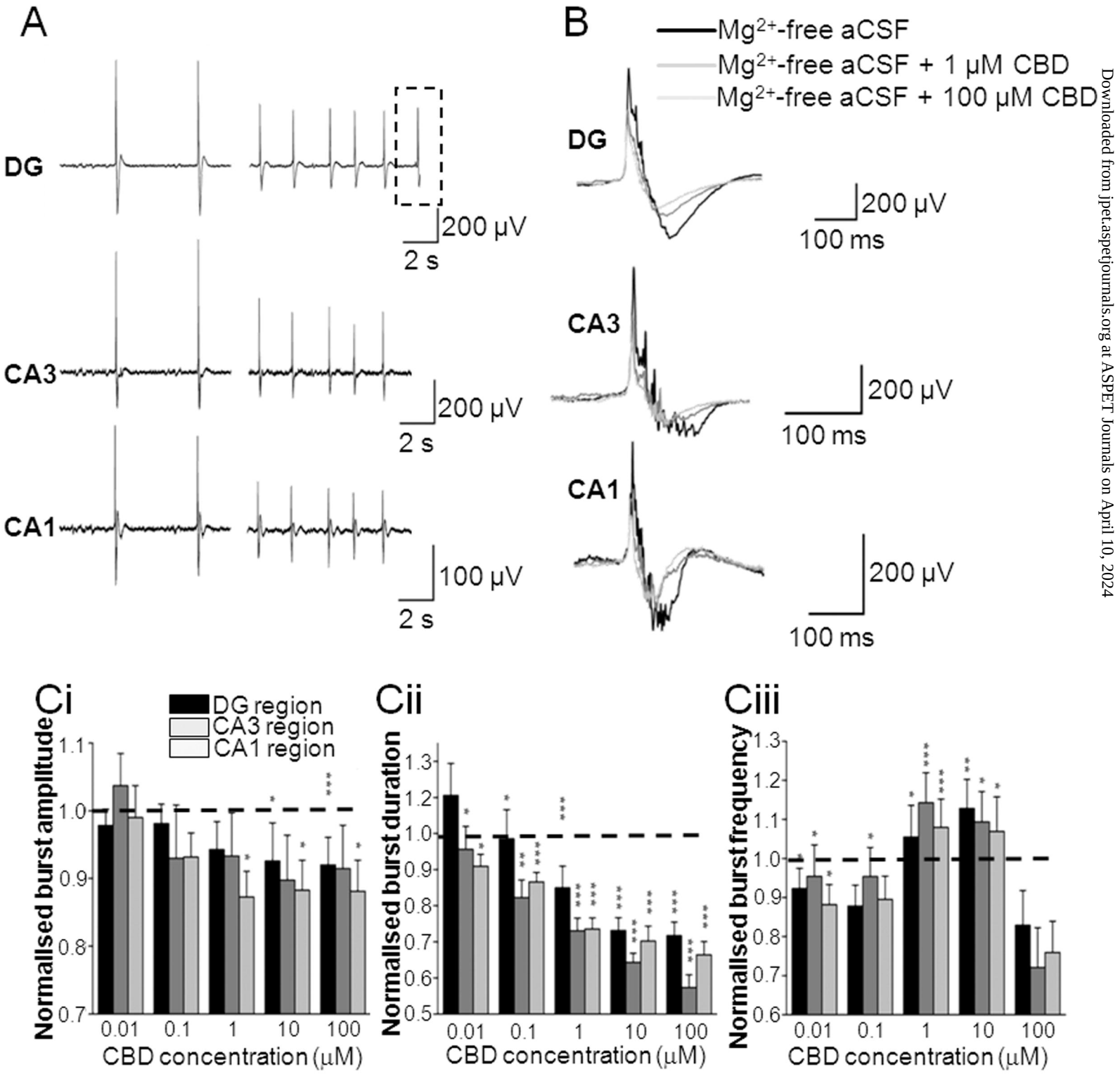

Figure 3

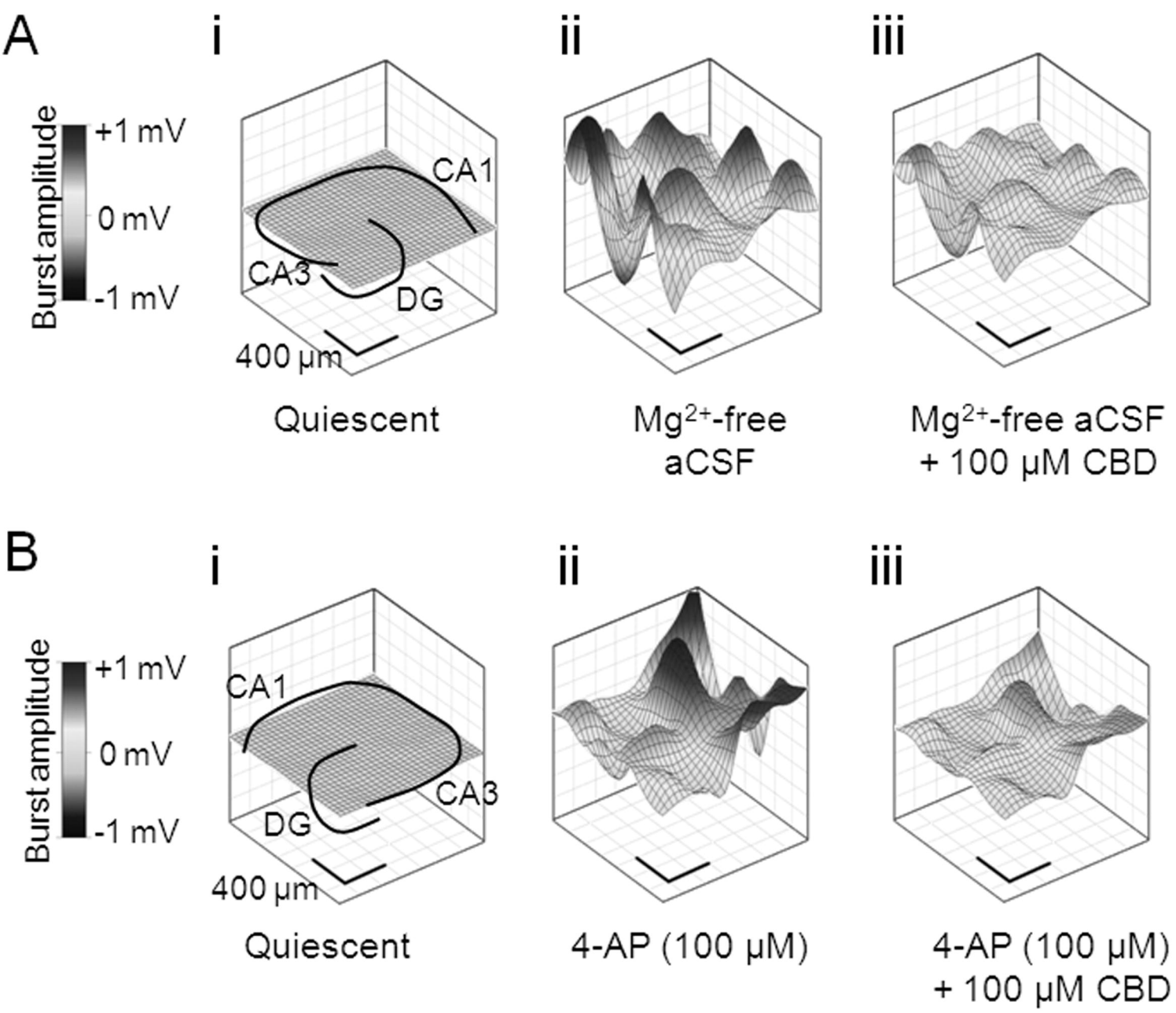

Figure 4

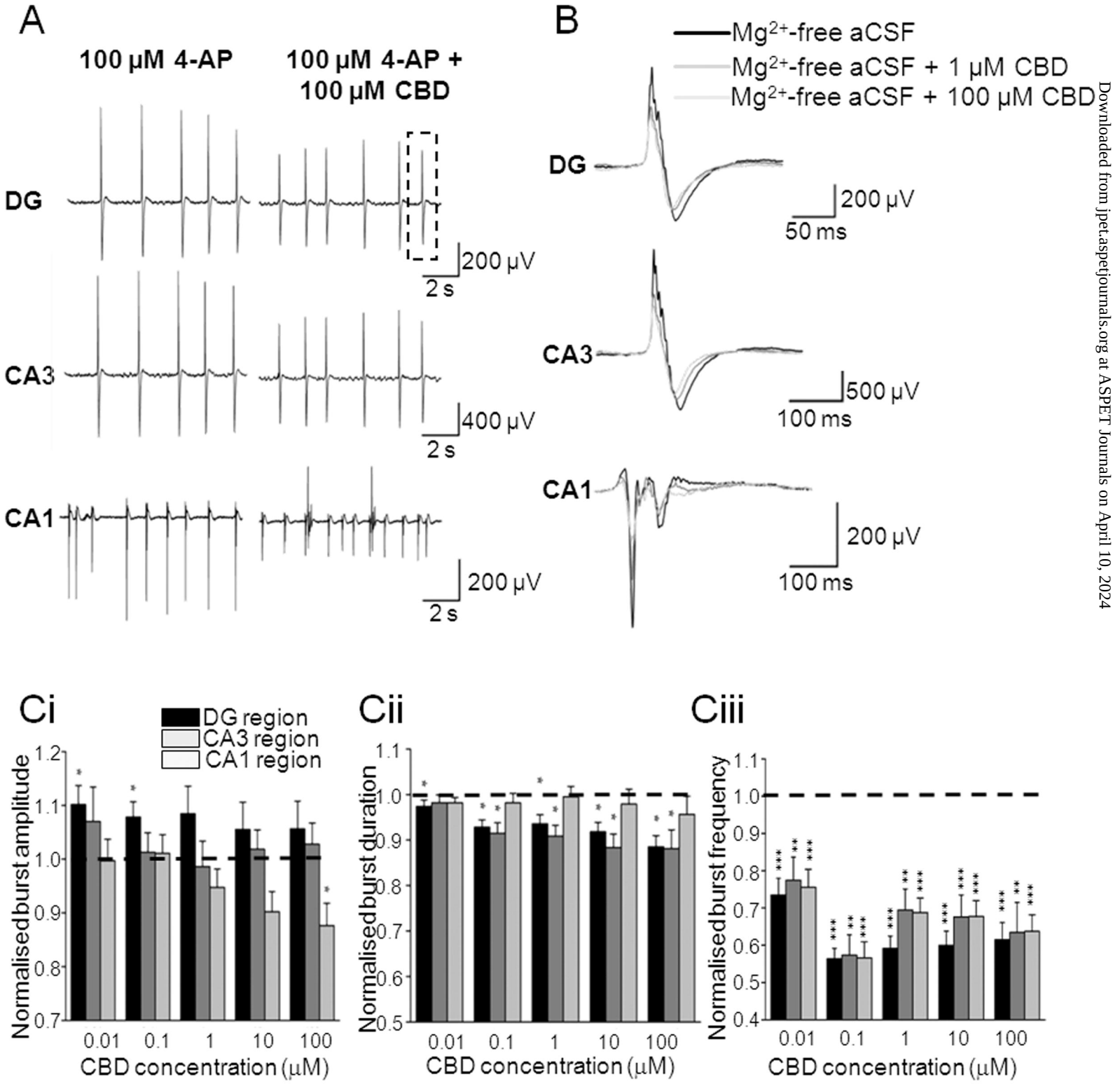

JPET Fast Forward. Published on November 11, 2009 as DOI: 10.1124/jpet.109.159145
This article has not been copyedited and formatted. The final version may differ from this version.

Figure 5

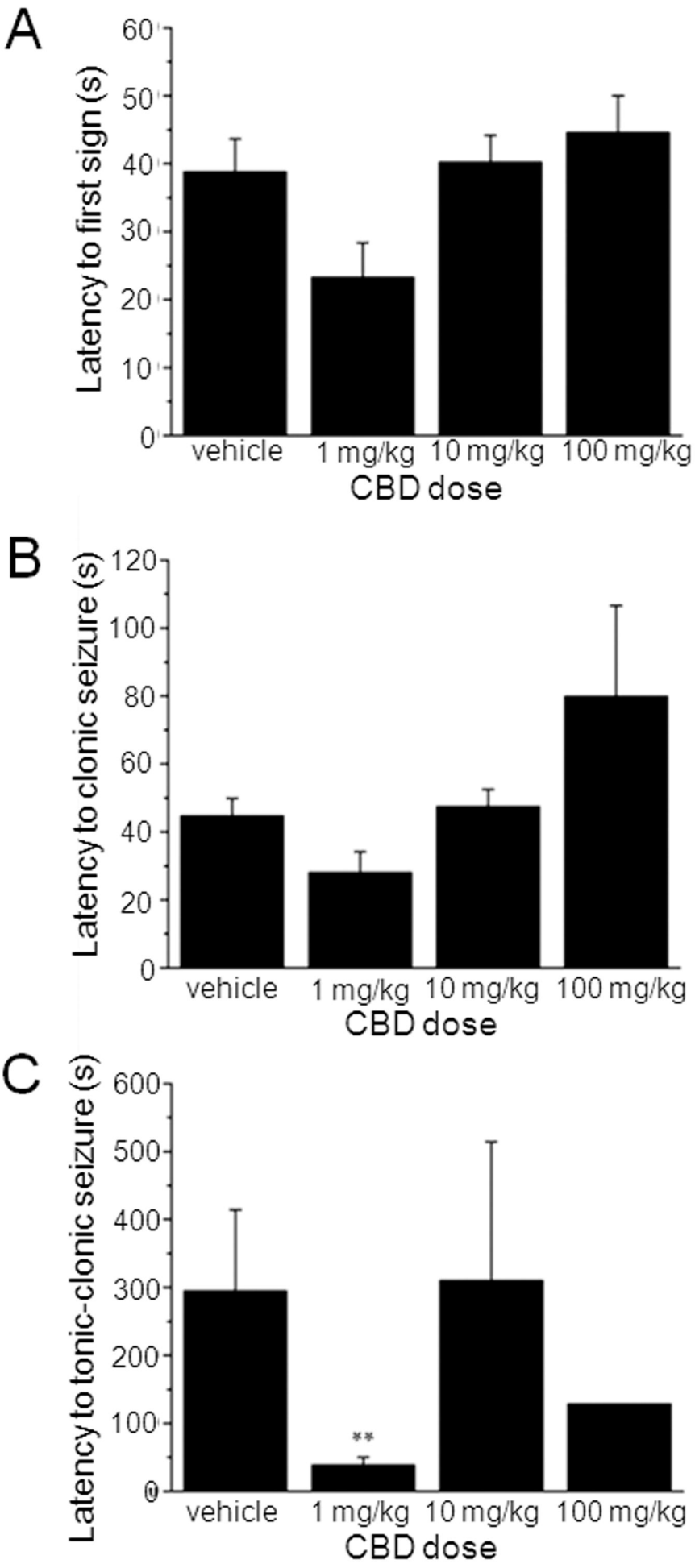

JPET Fast Forward. Published on November 11, 2009 as DOI: 10.1124/jpet.109.159145
This article has not been copyedited and formatted. The final version may differ from this version.

Figure 6

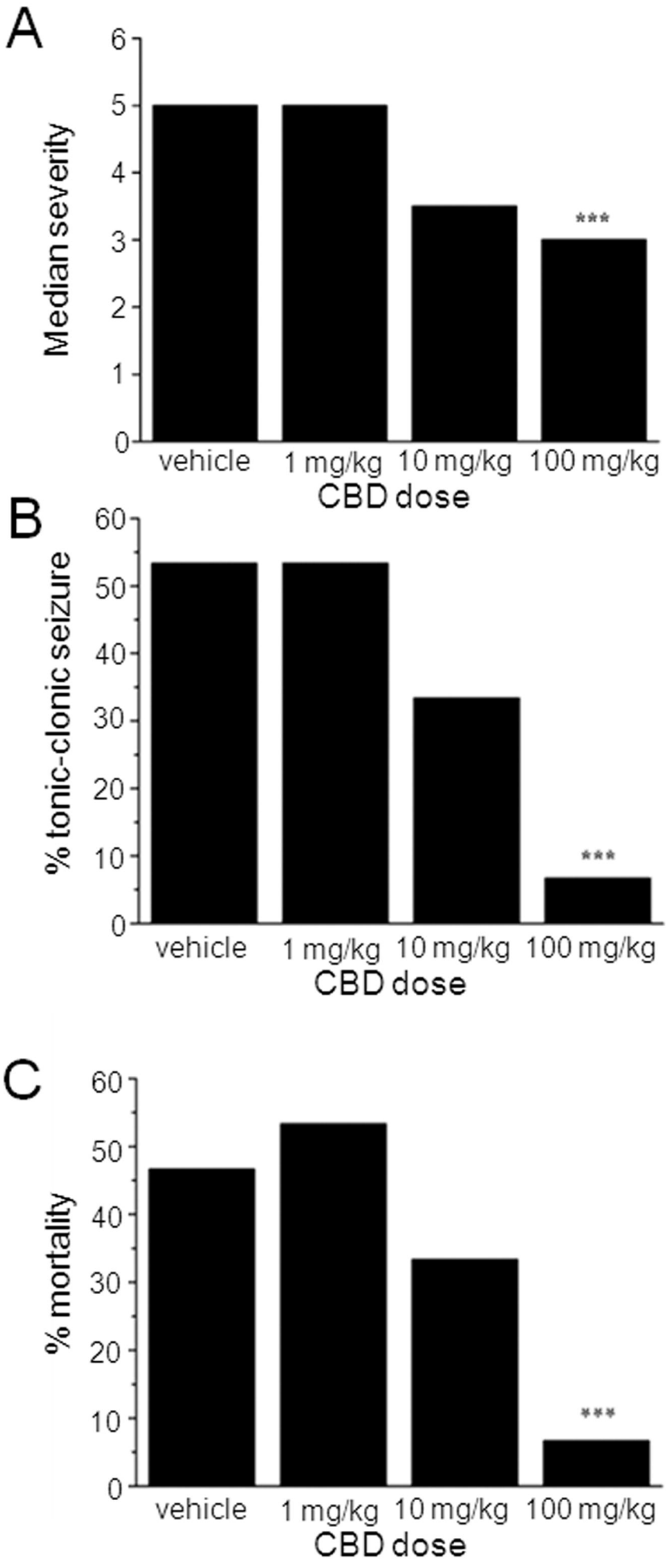

JPET Fast Forward. Published on November 11, 2009 as DOI: 10.1124/jpet.109.159145
This article has not been copyedited and formatted. The final version may differ from this version.

Figure 7